

# The Characteristic Length Scale of the Intermediate Structure in Zero-Pressure-Gradient Boundary Layer Flow

G. I. BARENBLATT,<sup>1</sup> A. J. CHORIN<sup>1</sup> AND V. M. PROSTOKISHIN<sup>2</sup>

<sup>1</sup>Department of Mathematics and  
Lawrence Berkeley National Laboratory  
University of California  
Berkeley, California 94720

<sup>2</sup>P. P. Shirshov Institute of Oceanology  
Russian Academy of Sciences  
36, Nakhimov Prospect  
Moscow 117218 Russia

## Abstract.

In a turbulent boundary layer over a smooth flat plate with zero pressure gradient, the intermediate structure between the viscous sublayer and the free stream consists of two layers: one adjacent to the viscous sublayer and one adjacent to the free stream. When the level of turbulence in the free stream is low, the boundary between the two layers is sharp and both have a self-similar structure described by Reynolds-number-dependent scaling (power) laws. This structure introduces two length scales: one — the wall region thickness — determined by the sharp boundary between the two intermediate layers, the second determined by the condition that the velocity distribution in the first intermediate layer be the one common to all wall-bounded flows, and in particular coincide with the scaling law previously determined for pipe flows. Using recent experimental data we determine both these length scales and show that they are close. Our results disagree with the classical model of the “wake region”.

# 1 Introduction

Turbulent boundary layer flow over a smooth flat plate outside a close vicinity of the plate tip contains two unambiguous elements: The viscous sublayer adjacent to the plate, where the velocity gradient is large and the viscous stress is comparable with the Reynolds stress, and the statistically uniform free stream.

According to classical theory [1], the region intermediate between these two consists of two layers with different properties. The first, adjacent to the viscous sublayer is a universal, Reynolds-number-independent logarithmic layer. In the second, the “wake region”, there is a smooth transition from the universal logarithmic layer to the free stream.

Our analysis of *all* available experiments [2–4] contradicts this classical theory. Indeed, in the clear-cut case of a smooth plate and low free stream turbulence, the intermediate structure does consist of two layers. However, the boundary between them is sharp. Most important, both layers are self-similar, substantially Reynolds-number-dependent, and described by different scaling laws. It is interesting to note (see the details below) that the same configuration of two self-similar layers with a sharp interface between them can be seen in all runs used in [1] for the illustration of the wake region model.

We found it possible [2–4] to introduce a characteristic length scale  $\Lambda$  so that the average velocity distribution in the first intermediate layer coincides with Reynolds-number-dependent scaling law obtained previously for pipe flows, when the Reynolds number is chosen as  $U\Lambda/\nu$ , with  $U$  the free stream velocity and  $\nu$  the fluid’s kinematic viscosity. The sharp boundary between the self-similar intermediate layers also defines a length scale  $\lambda$ . We show, by analysis of experimental data, that these two length scales  $\lambda$  and  $\Lambda$  are close.

## 2 Background

In a previous paper [2] we noted that when the turbulence level in the free stream is small, the intermediate structure between the viscous sublayer and the free stream consists of two self-similar layers: one adjacent to the viscous sublayer where the average velocity profile is described by the scaling law

$$\phi = A\eta^\alpha, \quad (2.1)$$

and one adjacent to the free stream where

$$\phi = B\eta^\beta. \quad (2.2)$$

Here

$$\phi = \frac{u}{u_*}, \quad u_* = \sqrt{\frac{\tau}{\rho}}, \quad \eta = \frac{u_* y}{\nu},$$

$u$  is the average velocity,  $\tau$  is the shear stress at the wall,  $\rho$  and  $\nu$  are the fluid density and kinematic viscosity;  $A, B, \alpha$  and  $\beta$  are Reynolds number dependent constants.

Our processing of all experimental data available in the literature [3,4] confirmed these observations and showed that it is always possible to find a length scale  $\Lambda$  so that, setting  $Re = U\Lambda/\nu$ , we can represent the scaling law (2.1) in the form

$$\phi = \left( \frac{1}{\sqrt{3}} \ln Re + \frac{5}{2} \right) \eta^{\frac{3}{2 \ln Re}} \quad (2.3)$$

obtained by us earlier for pipe flows (see, e.g. [5]). This suggests that *the structure of wall regions in all wall-bounded shear flows at large Reynolds numbers is identical, if the length scale and velocity scale are properly selected*. The natural question is, however, what is the physical meaning of this length scale  $\Lambda$  in boundary layer flow? This question is of substantial importance and should be clarified for proper understanding of the identity of scaling laws for different wall-bounded shear flows.

We note that the intermediate structure has another characteristic length scale  $\lambda$  — the wall-region thickness determined by the sharp intersection  $\eta = \eta_*$  of the two velocity distribution laws  $\phi = A\eta^\alpha$  and  $\phi = B\eta^\beta$  valid in the different layers. We have

$$A\eta_*^\alpha = B\eta_*^\beta, \quad (2.4)$$

so that

$$\eta_* = \left( \frac{A}{B} \right)^{\frac{1}{\beta-\alpha}}, \quad (2.5)$$

and the wall-region thickness  $\lambda$  is determined by the relation

$$\lambda = \left( \frac{A}{B} \right)^{\frac{1}{\beta-\alpha}} \frac{\nu}{u_*}. \quad (2.6)$$

On the other hand, the characteristic length scale  $\Lambda$  is determined by the relation

$$\Lambda = Re \frac{\nu}{U} = \left( \frac{u_*}{U} \right) \left( \frac{\nu}{u_*} \right) Re \quad (2.7)$$

so that the ratio of these two scales is

$$\frac{\Lambda}{\lambda} = \left( \frac{u_*}{U} Re \right) \frac{1}{\eta_*} = \left( \frac{u_*}{U} Re \right) \left( \frac{B}{A} \right)^{\frac{1}{\beta-\alpha}}. \quad (2.8)$$

### 3 Analysis of experimental data

We analyzed the recent data of J.M. Österlund presented on the Internet ([www.kth.se/~jens/zpg/](http://www.kth.se/~jens/zpg/)). The data seem to us to be reliable, however much we disagree with their processing and interpretation in the paper by Österlund et al [6] (see [4]). All 70 runs presented on the Internet give the characteristic broken-line average velocity distribution in  $\lg \eta, \lg \phi$  coordinates (see

the examples in Figure 1; all the other cases are similar), so that the possibility of determining  $A, \alpha, B, \beta$  and  $\eta_*$  accurately from these experimental data is unquestionable. These results are presented in Table 1 for all Österlund's experiments where  $Re_\theta = U\theta/\nu > 10,000$ . Here  $\theta$  is the momentum thickness; the runs in the Österlund's experimental data are labelled by  $Re_\theta$ .

The effective Reynolds number  $Re$  was obtained [4] by the formula

$$\ln Re = \frac{1}{2}(\ln Re_1 + \ln Re_2) \quad (3.9)$$

where  $\ln Re_1$  and  $\ln Re_2$  are the solutions of the equations

$$\frac{1}{\sqrt{3}} \ln Re_1 + \frac{5}{2} = A, \quad \frac{3}{2 \ln Re_2} = \alpha \quad (3.10)$$

and the values of  $A$  and  $\alpha$  were obtained by standard statistical processing of Österlund's data. For  $Re_\theta > 10,000$  the difference  $\delta$  between  $\ln Re_1$  and  $\ln Re_2$  does not exceed 3%, so that they coincide within experimental accuracy.

According to (2.7) and (2.8)

$$\lg \frac{\Lambda}{\lambda} = (\lg Re - \lg \eta_*) + \lg \frac{u_*}{U}. \quad (3.11)$$

The data for  $u_*$  and  $U$  are presented by Österlund on the Internet for each run. In Figure 2 we present the values of  $\lg(\Lambda/\lambda)$  for all runs. The mean value of  $\lg(\Lambda/\lambda)$  is approximately 0.2, so that the characteristic length scale  $\Lambda$  is about 1.6 times the thickness of the wall region.

If we take into account that  $\Lambda$  is calculated from the value of  $Re$ , and that  $\ln Re$ , not  $Re$  itself, has been determined from experiment, the ratios  $\Lambda/\lambda$  as shown in Figure 2 are close to unity.

We processed in [3,4] the data of 90 *zero-pressure-gradient* boundary layer experiments at low free stream turbulence performed by different authors during the last 25 years — all the experiments of this kind available to us. Without exception, all runs revealed identical configurations of the intermediate structure in the boundary layer: two adjacent self-similar layers separated by a sharp interface.

According to the classical model [1], the intermediate structure consists of the (universal) logarithmic layer and a non-self-similar “wake region” smoothly matching the logarithmic layer. It was natural to also process the very data used in [1] for the justification of the wake region model with the general procedure we used on the other data. The data presented in Figure 21 of [1] were scanned and replotted in  $\lg \eta, \lg \phi$  coordinates as was done for all experimental data processed in [3,4]. Processing revealed the same broken-line structure, i.e. two adjacent self-similar layers (see Table 2 and Figure 3, where a typical example is presented). The difference between  $\ln Re_1$  and  $\ln Re_2$  determined from the wall layer data is small: this shows that the procedure is adequate. We conjecture that the values of  $\beta$  are larger than in newer experiments because of a non-zero pressure gradient in all these runs (see [1]). The results of our processing fail to confirm the wake region model proposed in [1].

## 4 Conclusion

We have shown that one can find a length scale  $\Lambda$  so that, if the Reynolds number  $Re$  in a zero-pressure-gradient boundary layer flow is defined by  $Re = U\Lambda/\nu$ , with  $U$  the free stream velocity and  $\nu$  the kinematic viscosity, then the scaling law for the self-similar region adjacent to the viscous sublayer coincides with the scaling law for turbulent pipe flow. Using the recent experimental data of Österlund ([www.kth.se/~jens/zpg/](http://www.kth.se/~jens/zpg/)) we confirmed this fact and reached the important conclusion that  $\Lambda$  is roughly equal to the wall-region thickness. Our results are in disagreement with the classical model of the wake region in the boundary layer [1].

**Acknowledgments.** This work was supported in part by the Applied Mathematics subprogram of the U.S. Department of Energy under contract DE-AC03-76-SF00098, and in part by the National Science Foundation under grants DMS 94-16431 and DMS 97-32710.

## References

1. Coles, D. (1956). *J. Fluid Mech.* **1**, pp.191–226.
2. Barenblatt, G.I., Chorin, A.J., Hald, O. and Prostokishin, V.M. (1997). *Proceedings National Academy of Sciences USA* **94**, pp.7817–7819.
3. Barenblatt, G.I., Chorin, A.J., and Prostokishin, V.M. (2000). *J. Fluid Mech.*, in press.
4. Barenblatt, G.I., Chorin, A.J., and Prostokishin, V.M. (2000). Analysis of experimental investigations of self-similar structures in zero-pressure-gradient boundary layers at large Reynolds numbers. Center for Pure & Applied Mathematics, UC Berkeley, CPAM-777.
5. Barenblatt, G.I., Chorin, A.J., and Prostokishin, V.M. (1997). *Applied Mechanics Reviews*, vol. **50**, no. 7, pp.413–429.
6. Österlund, J.M., Johansson, A.V., Nagib, H.M. and Hites, M.H. (2000). *Physics of Fluids*, vol. **12**, no. 1, pp.1–4.

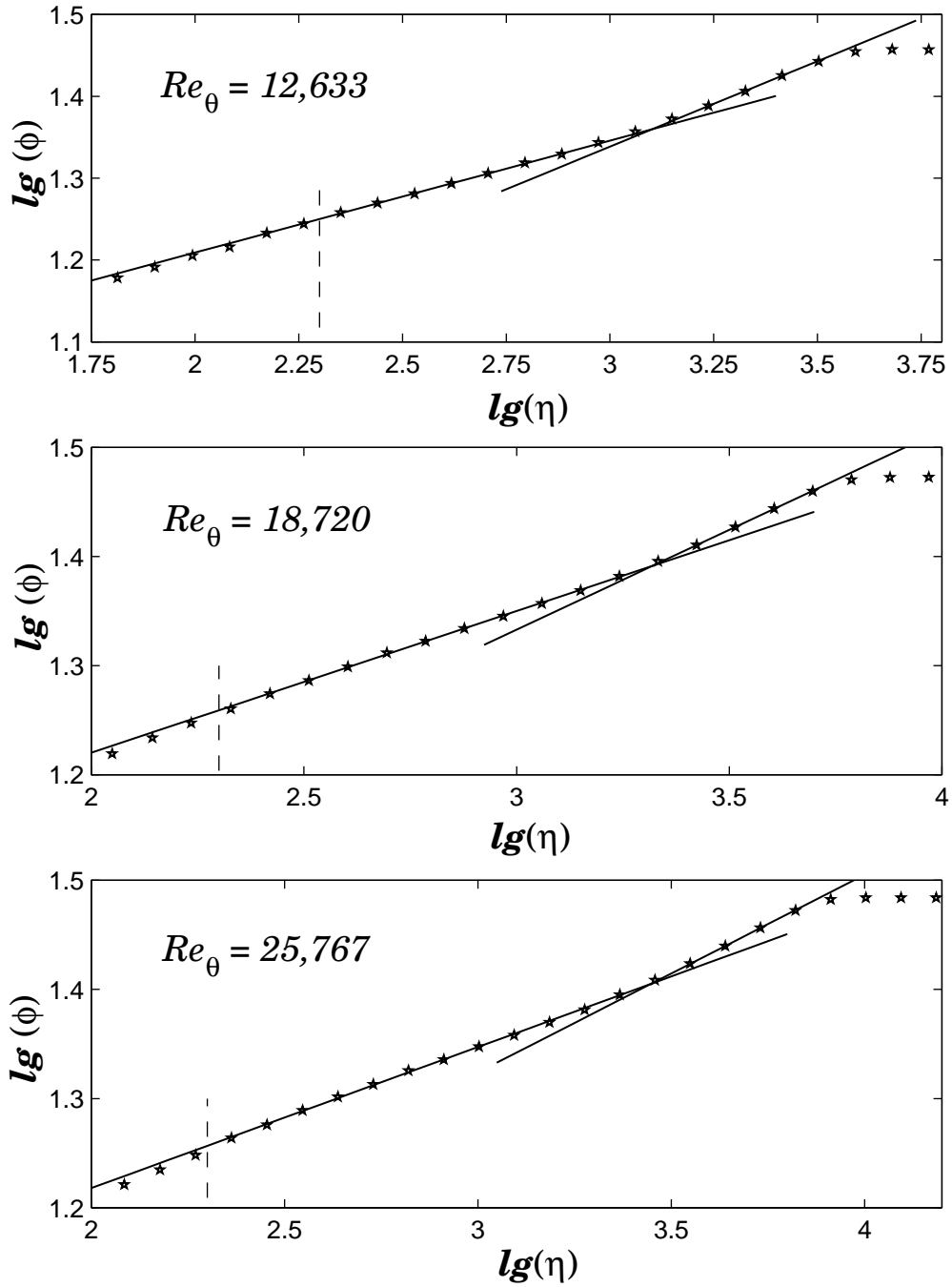


Figure 1.

Table1

Re $\theta$	$\alpha$	A	$\beta$	B	ln(Re1 )	ln(Re2 )	ln(Re)	$\delta$	U	u*	$\eta^*$
10 161	0.142	8.43	0.196	5.82	10.27	10.54	10.41	2.5%	53.71	1.91	1.0 E+3
10 313	0.140	8.51	0.202	5.53	10.41	10.74	10.58	3.0%	37.44	1.33	1.1 E+3
10 386	0.139	8.58	0.204	5.45	10.53	10.81	10.67	2.6%	21.21	0.75	1.1 E+3
10 502	0.141	8.38	0.204	5.44	10.18	10.62	10.40	4.2%	27.00	0.96	9.9 E+2
11 733	0.139	8.56	0.199	5.57	10.50	10.77	10.63	2.5%	42.75	1.50	1.2 E+3
12 150	0.140	8.48	0.199	5.56	10.36	10.69	10.53	3.1%	21.42	0.75	1.2 E+3
12 239	0.139	8.55	0.200	5.50	10.47	10.79	10.63	3.0%	32.40	1.14	1.3 E+3
12 308	0.137	8.67	0.202	5.46	10.69	10.98	10.83	2.6%	21.23	0.74	1.2 E+3
12 633	0.137	8.61	0.209	5.16	10.59	10.96	10.77	3.4%	21.42	0.75	1.3 E+3
12 866	0.134	8.88	0.193	5.81	11.05	11.22	11.13	1.5%	47.93	1.67	1.3 E+3
12 886	0.137	8.65	0.200	5.52	10.65	10.95	10.80	2.7%	26.91	0.94	1.3 E+3
13 878	0.137	8.69	0.196	5.63	10.73	10.99	10.86	2.4%	37.74	1.31	1.4 E+3
14 207	0.132	9.01	0.191	5.87	11.28	11.39	11.33	1.0%	26.54	0.92	1.4 E+3
14 289	0.132	9.02	0.188	5.98	11.29	11.39	11.34	0.9%	53.16	1.84	1.5 E+3
14 972	0.134	8.81	0.198	5.51	10.92	11.16	11.04	2.2%	32.37	1.11	1.6 E+3
15 164	0.134	8.80	0.199	5.45	10.91	11.19	11.05	2.6%	26.90	0.92	1.5 E+3
15 182	0.130	9.03	0.199	5.45	11.32	11.53	11.42	1.9%	26.75	0.92	1.5 E+3
15 512	0.129	9.14	0.189	5.91	11.50	11.61	11.56	1.0%	43.02	1.48	1.7 E+3
16 422	0.131	9.08	0.185	6.05	11.39	11.43	11.41	0.3%	31.67	1.08	1.8 E+3
17 102	0.134	8.87	0.188	5.91	11.04	11.23	11.13	1.7%	37.81	1.29	1.8 E+3
17 279	0.129	9.15	0.187	5.95	11.52	11.62	11.57	0.8%	48.37	1.64	1.9 E+3
17 813	0.129	9.11	0.191	5.73	11.45	11.63	11.54	1.6%	32.41	1.10	1.9 E+3
17 901	0.135	8.75	0.196	5.51	10.82	11.12	10.97	2.7%	32.21	1.09	1.8 E+3
18 479	0.127	9.38	0.178	6.35	11.91	11.85	11.88	0.5%	36.74	1.24	2.0 E+3
18 720	0.126	9.34	0.183	6.08	11.85	11.87	11.86	0.2%	53.63	1.81	2.0 E+3
19 235	0.126	9.33	0.187	5.89	11.83	11.89	11.86	0.5%	43.26	1.46	1.9 E+3
20 258	0.127	9.25	0.188	5.81	11.69	11.80	11.75	0.9%	37.40	1.25	2.0 E+3
20 562	0.130	9.08	0.186	5.93	11.40	11.57	11.48	1.5%	37.88	1.27	2.0 E+3
20 958	0.125	9.44	0.180	6.16	12.02	12.03	12.02	0.1%	48.68	1.63	2.3 E+3
21 099	0.125	9.42	0.180	6.17	11.98	12.00	11.99	0.1%	40.00	1.34	2.1 E+3
22 579	0.123	9.54	0.179	6.19	12.19	12.16	12.18	0.3%	52.61	1.75	2.4 E+3
22 845	0.126	9.34	0.184	5.95	11.86	11.94	11.90	0.7%	42.51	1.41	2.3 E+3
23 119	0.123	9.52	0.177	6.28	12.16	12.15	12.15	0.1%	45.35	1.50	2.3 E+3
23 309	0.129	9.11	0.184	5.93	11.44	11.64	11.54	1.7%	43.57	1.44	2.3 E+3
23 870	0.121	9.70	0.177	6.30	12.46	12.42	12.44	0.4%	46.45	1.53	2.3 E+3
25 767	0.124	9.42	0.181	6.04	11.99	12.08	12.04	0.7%	49.11	1.61	2.5 E+3
25 779	0.125	9.30	0.187	5.74	11.79	11.96	11.87	1.5%	48.29	1.58	2.7 E+3
26 612	0.120	9.74	0.177	6.24	12.54	12.48	12.51	0.5%	52.18	1.71	2.7 E+3
27 320	0.124	9.54	0.173	6.42	12.20	12.13	12.17	0.6%	54.04	1.76	3.0 E+3

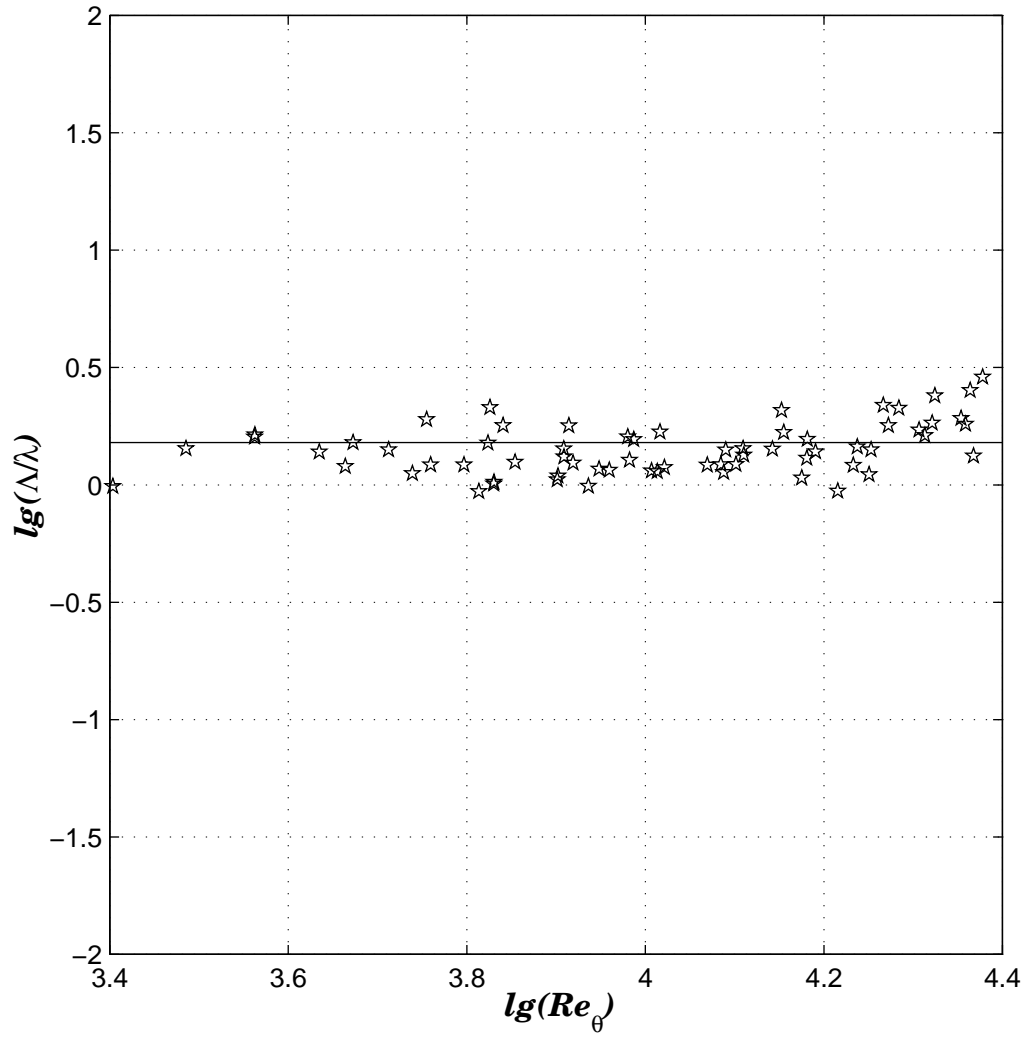


Figure 2.

**Table 2**

<b>N</b>	<b><math>\alpha</math></b>	<b>A</b>	<b><math>\beta</math></b>	<b>B</b>	<b>ln(Re1)</b>	<b>ln(Re2)</b>	<b>ln(Re)</b>	<b><math>\delta</math></b>
<b>1</b>	<b>0.163</b>	<b>7.90</b>	<b>0.70</b>	<b>0.42</b>	<b>9.35</b>	<b>9.18</b>	<b>9.27</b>	<b>2%</b>
<b>2</b>	<b>0.176</b>	<b>7.29</b>	<b>0.51</b>	<b>0.82</b>	<b>8.30</b>	<b>8.55</b>	<b>8.43</b>	<b>3%</b>
<b>3</b>	<b>0.180</b>	<b>7.17</b>	<b>0.56</b>	<b>0.66</b>	<b>8.09</b>	<b>8.34</b>	<b>8.22</b>	<b>3%</b>
<b>4</b>	<b>0.171</b>	<b>7.43</b>	<b>0.57</b>	<b>0.60</b>	<b>8.55</b>	<b>8.75</b>	<b>8.65</b>	<b>3%</b>
<b>5</b>	<b>0.185</b>	<b>6.77</b>	<b>0.64</b>	<b>0.30</b>	<b>7.41</b>	<b>8.11</b>	<b>7.76</b>	<b>9%</b>
<b>6</b>	<b>0.151</b>	<b>8.20</b>	<b>0.55</b>	<b>0.49</b>	<b>9.87</b>	<b>9.96</b>	<b>9.92</b>	<b>1%</b>
<b>7</b>	<b>0.158</b>	<b>7.71</b>	<b>0.50</b>	<b>0.67</b>	<b>9.02</b>	<b>9.52</b>	<b>9.27</b>	<b>6%</b>

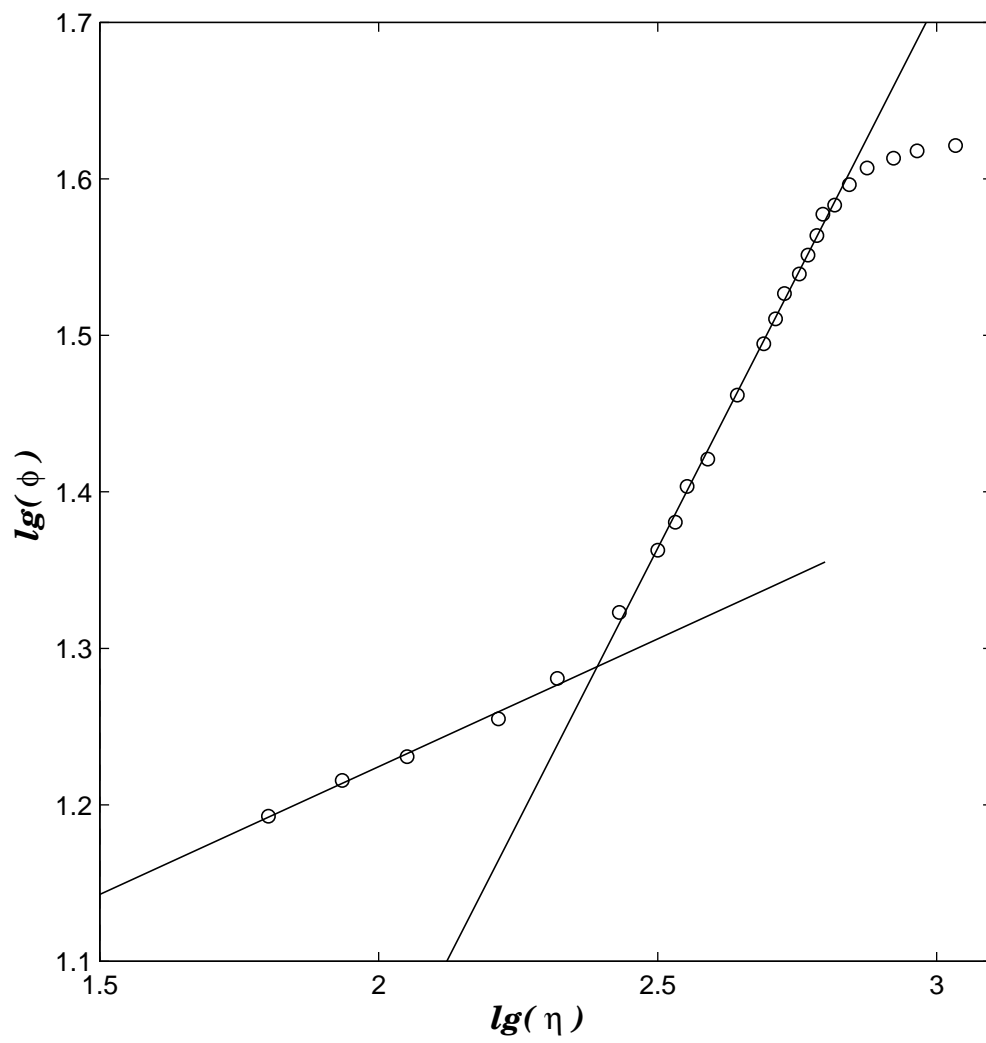


Figure 3.